

Article

Stress and Fatigue Analysis of Picking Device Gears for a 2.6 kW Automatic Pepper Transplanter

Md Nafiul Islam ^{1,2}, Md Zafar Iqbal ³, Milon Chowdhury ^{1,2}, Mohammad Ali ¹, Kiraga Shafik ²,
Md Shaha Nur Kabir ⁴, Dae-Hyun Lee ^{1,2} and Sun-Ok Chung ^{1,2,*}

- ¹ Department of Agricultural Machinery Engineering, Graduate School, Chungnam National University, Daejeon 34134, Korea; nafiulislam@cnu.ac.kr (M.N.I.); chowdhurym90@cnu.ac.kr (M.C.); sdali77@o.cnu.ac.kr (M.A.); leedh7@cnu.ac.kr (D.-H.L.)
- ² Department of Smart Agricultural Systems, Graduate School, Chungnam National University, Daejeon 34134, Korea; kiragashafik@o.cnu.ac.kr
- ³ Department of Biological and Agricultural Engineering, College of Agriculture and Life Sciences, Texas A&M University, College Station, TX 77843, USA; z_iqbal@tamu.edu
- ⁴ Department of Agricultural and Industrial Engineering, Faculty of Engineering, Hajee Mohammad Danesh Science and Technology University, Dinajpur 5200, Bangladesh; kabir1982@hstu.ac.bd
- * Correspondence: sochung@cnu.ac.kr; Tel.: +82-42-821-6712; Fax: +82-42-823-6246

Abstract: A seedling picking device is an essential component for an automatic transplanter to automatically convey the seedling to the dibbling part. It is necessary to find the appropriate material and dimensions for the picking device gears to avoid mechanical damage and increase their durability. Therefore, the objectives of this research were to analyze the stress of a picking device gear mechanism in order to select suitable materials and dimensions, and to predict the fatigue life by considering the damage level. The picking device gear shaft divided the input power into two categories, i.e., crank and cam gear sets. Finite element analysis simulation and American Gear Manufacturers Association standard stress analysis theory tests were conducted on both of the crank and cam gear sets for different materials and dimensions. A test bench was fabricated to collect the load (torque) data at different gear operating speeds. The torque data were analyzed using the load duration distribution method to observe the cyclic load patterns. The Palmgren–Miner cumulative damage rule was used to determine the damage level of the picking mechanism gears with respect to the operating speed. The desired lifespan of the transplanter was 255 h to meet the real field service life requirement. Predicted fatigue life range of the picking mechanism gears was recorded as from 436.65 to 4635.97 h, making it higher (by approximately 2 to 18 times) than the lifespan of the transplanter. According to the analyses, the “Steel Composite Material 420H carbon steel” material with a 5 mm face width gear was suitable to operate the picking device for a 10-year transplanter service life. The analysis of stress and fatigue presented in this study will guide the design of picking device gears with effective material properties to maintain the recommended service life of the pepper transplanter.

Keywords: agricultural machinery; pepper transplanting; seedling picking mechanism; structural analysis; gear mechanism; assessment of stress and fatigue



Citation: Islam, M.N.; Iqbal, M.Z.; Chowdhury, M.; Ali, M.; Shafik, K.; Kabir, M.S.N.; Lee, D.-H.; Chung, S.-O. Stress and Fatigue Analysis of Picking Device Gears for a 2.6 kW Automatic Pepper Transplanter. *Appl. Sci.* **2021**, *11*, 2241. <https://doi.org/10.3390/app11052241>

Academic Editor: Esteban Rougier

Received: 8 February 2021

Accepted: 26 February 2021

Published: 3 March 2021

Publisher's Note: MDPI stays neutral with regard to jurisdictional claims in published maps and institutional affiliations.



Copyright: © 2021 by the authors. Licensee MDPI, Basel, Switzerland. This article is an open access article distributed under the terms and conditions of the Creative Commons Attribution (CC BY) license (<https://creativecommons.org/licenses/by/4.0/>).

1. Introduction

Peppers (*Capsicum annuum* L.) are the most commonly consumed type of spicy vegetable and the second most commonly traded vegetable worldwide [1,2]. Although pepper production is increasing globally, decreased rates were recorded in some countries (e.g., Korea and Japan) over the last few decades due to farm labor shortages, small agricultural land areas, and the aging of farmers [3]. Therefore, to reduce the labor requirement and the difficulty of operation of the pepper transplanting operation, mechanical transplanters have increased in popularity [4]. Furthermore, to achieve an easier and more farmer-friendly mechanical pepper transplanting technique, researchers have focused on designing fully

automated transplanting operations. A picking device is an essential part of an automatic transplanter as it reduces the difficulty of operation by carrying out a repetitive task in a precise and consistent manner [3]. For favorable structural durability and manufacturing costs, the assessment of stress and fatigue damage is a crucial stage before operation at the agricultural field level [5].

The structural durability requirements of a machine can be satisfied if the machine parts are designed to have an adequate fatigue strength based on the service life [6,7]. The most critical design conditions for the machine are the material and dimension requirements, since some components may experience excessive loads [8,9]. Among the major components of a machine, critical loading conditions occur in the transmission system, such as gears and gear shafts [10]. Generally, in the gear mechanism, immediate load variation occurs in relation to the mechanical transmission, particularly at teeth contact points [11,12]. Researchers have suggested various approaches, including a simulation-based finite element analysis (FEA), for calculating the load distribution and stress of the gear set [13–17]. Based on these studies, the contact stress analysis of the gear mechanism could estimate the necessary gear dimension and material properties and play a significant role in evaluating the damage to the machine in the development and performance evaluation stages. Hwang et al. [16] investigated the gear contact stress during rotation at various contact positions. The roll angle was used to measure the contact positions and evaluated the FEA results for the specific position. Park et al. [17] classified different types of gear faults by analyzing the ensemble empirical mode decomposition to the transmission error and found the criteria of maximum gear fault by applying the FEA method. For a single pair of teeth, the stress was determined at the contact surface between two spheres at different loads and speed, based on the theoretical analysis [12]. In the simulation-based study, several strengths were used in terms of management time and costs, but if the real working environmental conditions were not reflected, it was challenging to ensure the consistency of the results [18]. Load measurement experiments were required to validate the simulation-based study by determining the damage level for the selected gear dimensions and material properties.

Load analysis and fatigue life prediction based on the designated gear dimension and material are important for safety, preventing damage, and ensuring the structural reliability of the picking operation. Several methods have been examined to enhance the fatigue life prediction accuracy for different types of machinery [19]. In 1936, Kloth and Stoppel [20] formulated a structural durability test for agricultural machinery (binding mower), analyzing the applied load in a real field. The structural durability under field conditions for a rotary cultivator was examined by Harral [21]. Previously, research on load analysis through field investigations has mainly focused on fundamental statistical analyses [18]. Recently, researchers have focused on creating a spectrum [22,23] and evaluating relative severity [24–26] and damage level [27,28] to ensure the safety and reliability of agricultural machines. Kim et al. [26] studied the transmission loads at the gear mechanism input shaft during various operations such as rotary tillage, plow tillage, and crop transportation operations. Lee et al. [25] examined a tractor power take-off (PTO) gear according to the engine power for the optimum powertrain design. The experimental results showed that the tractor PTO could perform at a lower level than the minimum output of the engine, and this reduced the fatigue life of the PTO gear. All possible loads during different operating modes, the total amount of h per year, and the total amount of years of the mechanism's life were considered to evaluate the fatigue life.

An automatic pepper transplanter is currently under development, and the major applied load part (gears) of the picking device needs to be evaluated in terms of the mechanical properties and fatigue life to successfully operate the transplanter within a satisfactory service life range. Therefore, the objectives of this research were to analyze the stress condition of the picking device gear mechanism for determining the gear dimensions and material using a simulation-based FEA and theoretical method, and to predict the fatigue life of the gear mechanism by analyzing the damage level in terms of the load acting on the gear for different operating speeds.

2. Materials and Methods

2.1. Structure of the Automatic Pepper Transplanter under Development

The overall structure of the automated pepper transplantation device under development, which includes a picking mechanism, is shown in Figure 1. The pepper transplanter consists of three main devices: a picking device (a), a conveying device (b), and a dibbling device (c). A two-row pepper seedling dibbling device is attached to the conveying unit to plant the seedlings. The picking device picks five seedlings simultaneously from the tray and transfers them to the conveying unit. The conveying unit drops seedlings into the two-row, hopper-type dibbling devices by rotating the sprocket and chain. A 2.6 kW engine (SUBARU Industrial Products Co. Ltd., Ōta, Japan) was used as the prime mover of the transplanter. The picking mechanism uses two gear sets to move the pepper seedlings from the tray to the conveying unit. The two sets of spur gear trains are attached to the gear shaft with a 1:1 gear ratio for crank and 2:1 gear ratio for cam. The input power is provided from the engine, and the load is distributed on the gears. Gearing is the most efficient method for transmitting mechanical power from one shaft to another, with or without changing the speed [10,12]. The gear load was assumed to be distributed along the contact line of the contact gears. The gear contact point position changes the load distribution level. For the gear mechanism, a stress and fatigue analysis of the gears can be used to predict stress condition and service life, in terms of the maximum load distribution and fluctuations of a certain number of loads.

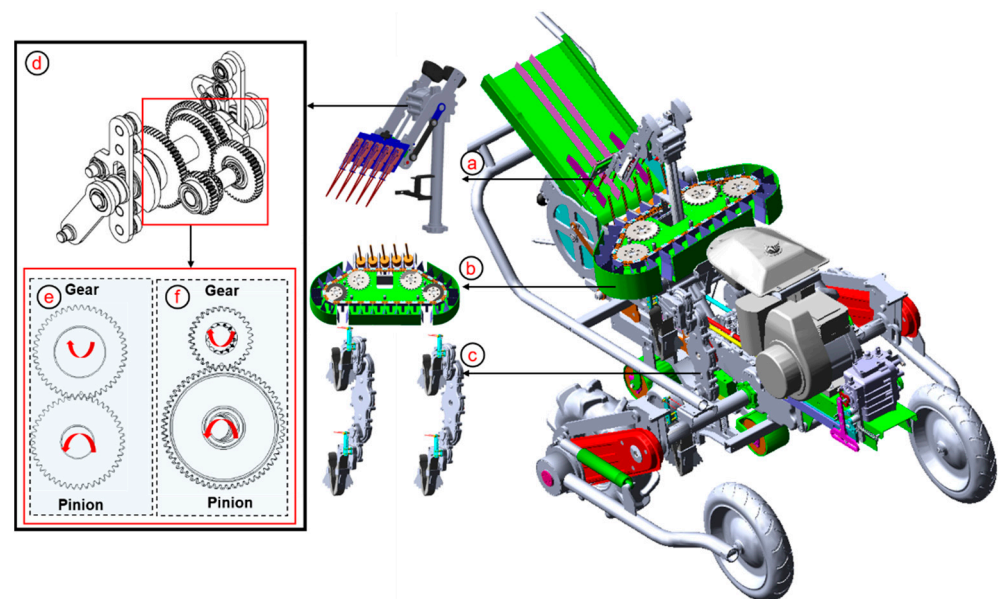


Figure 1. The overall structure of the automatic pepper transplanter under development: (a) picking device, (b) conveying device, (c) dibbling device, (d) picking gear mechanism, (e) crank gear set, and (f) cam gear set.

2.2. Determination of Suitable Face Width and Material

Gear tooth breakage or operation above the limit of the contact teeth durability harms the service life of a gear mechanism. Determination of a reasonable face width range is important to avoid micropitting of the contact teeth [29]. In this study, after selecting the face width range, an FEA simulation was performed to select the maximum stress position by applying a gear mechanism load in terms of the contact teeth, contact ratio, and roll angle [17]. A theoretical method considering the American Gear Manufacturers Association (AGMA) theory was used to evaluate the FEA simulation and determine a suitable face width and material. Figure 2 shows the stress analysis procedure of the picking device gear to determine the dimension (face width) and material. Table 1 indicates the considered variables in the stress and fatigue analysis of the picking device.

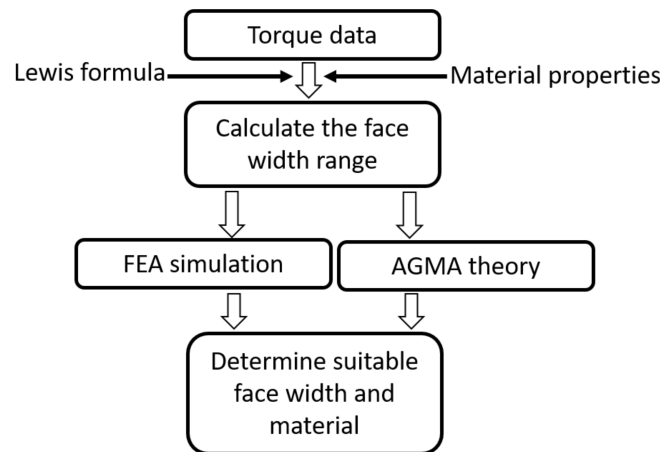


Figure 2. Block diagram showing the procedure to determine suitable gear set face width and material. AGMA: American Gear Manufacturers Association; FEA: finite element analysis.

Table 1. Variable notations, definitions, and units for picking device stress and fatigue analysis.

| Notation | Definition, Unit and Value |
|-------------|---|
| σ | Material allowable stress, MPa |
| k_v | Velocity factor, integer |
| w_t | Full gear load, MPa |
| F | Face width, m |
| m | Gear module, m |
| Y | Lewis factor, integer |
| V | Velocity, m/s |
| d | Gear diameter, m |
| N | Rotational speed, rad/s |
| l | Length of the line of action, m |
| r_{o1} | Gear addendum circle radius, m |
| r_{b1} | Gear base circle radius, m |
| r_{o2} | Pinion addendum circle radius, m |
| r_{b2} | Pinion base circle radius, m |
| r_{p1} | Gear radius of the pitch circle, m |
| r_{p2} | Pinion radius of the pitch circle, m |
| θ | Pressure angle, rad |
| P_b | Base circle, m |
| P_n | Pitch circle, m |
| φ_C | Roll angle, rad |
| φ_A | The angle of approach, rad |
| φ_R | The angle of recess, rad |
| S_A | Positions of the starting points |
| S_B | Positions of the endpoints |
| F_m | Nominal tangential force at mid-face width, N |
| T | Torque, Nm |
| d_m | Mean pitch diameter of the gear and pinion, m |
| σ_H | Teeth contact stress, MPa |
| Z_E | Elastic coefficient, MPa |
| K_o | Overload factor, 1.5 |
| K_d | Dynamic factor, 1 |
| K_s | Size factor, 1 |
| K_H | Load distribution factor, 1 |
| Z_1 | Geometry factor for pitting resistance |
| N_T | Total number of load cycles |
| D_i | Duration at <i>i</i> th bin, s |
| D_t | Total duration, s |
| N_i | Rotational speed at <i>i</i> th bin, rad/s |

Table 1. *Cont.*

| Notation | Definition, Unit and Value |
|----------|--|
| L | Lifespan of transplanter, years |
| N | Number of cycles, integer |
| D | Damage sum, integer |
| n_i | Number of cycles of measured data at the i th stress level |
| N_c | Number of cycles of the S–N curve at the i th stress level |
| L_f | Predicted fatigue life, h |
| L_s | The service life of the tractor, h |
| C_f | Predicted fatigue life cycles, integer |

2.2.1. Selection of Appropriate Face Width Range

The gear tooth is considered as an individual cantilever beam during load transmission; it is subjected to bending or winding [30]. The average gear load is tangential, applied at the midpoint along the face width, and considered for calculation of bending stress [31]. Using the Lewis formula, the properties of the material and the acting load of the gear were estimated using the gear face width [32]. The bending stress in a gear tooth was calculated using the Lewis bending stress theory, as shown in Equation (1). This theory describes the gear teeth as a simple cantilever beam, which experiences the full load [32].

$$\sigma = \frac{k_v w_t}{F m y} \quad (1)$$

$$k_v = \frac{3.05 + V}{3.05} \text{ (cast profile) and } V = \pi d N \quad (2)$$

The preferred face width of the gear depends on the allowable stress for the material. In gear design, steel materials are used to make the spur gears, as recommended by many researchers [33–35]. Several types of carbon steel are available at the research and field level; among them, two of the most commonly used, “Steel Composite Material (SCM) 420H carbon steel (medium carbon steel)” and “American Iron and Steel Institute (AISI) 1060 steel (high carbon steel)”, were selected for this analysis. A suitable range for the face width needs to be selected with consideration of the allowable stress, endurance limit, and factor of safety of the materials used for the gear sets. The properties of the selected gear materials are shown in Table 2.

Table 2. Material properties of the gear used for stress analysis.

| Material | Poisson Ratio | Modulus of Elasticity, MPa | Tensile Strength, MPa | Endurance Limit, MPa |
|--------------------------------|---------------|----------------------------|-----------------------|----------------------|
| Medium-carbon steel (SCM 420H) | 0.30 | 210 | 1158 | 579 |
| High-carbon steel (AISI 1060) | 0.29 | 212 | 1105 | 552.50 |

2.2.2. Gear Contact Stress Analysis by FEA Simulation

An FEA software package (midas NFX–2019, MIDAS Information Technology Co. Ltd., Seongnam, Korea) was used to estimate the contact stress and determine the maximum stress location in the picking device gears by FEA numerical simulation. The gear sets were assumed to make of SCM 420H carbon steel (medium carbon steel) or AISI 1060 steel (high carbon steel). The outline of the gear set tooth was divided into involute and trochoid curves. First, it is necessary to identify the gear set tooth that has an involute gear tooth outline. If gear parameters such as the module, teeth number, pressure angle, and radius of pitch circle are specified, the involute gear tooth outline can be determined using the gear parameters and function of the involute curve [16].

Before starting the FEA simulation, the individual three-dimensional crack and cam gear set geometry were generated. The general contact assembly was used to make contact

between the master (gear) and slave (pinion). For the assembly discretization and stress distribution, the three-dimensional geometry was meshed using mapped face meshing to obtain a uniform mesh structure. After completing the mesh, the boundary conditions, including self-weight, displacement, supports, loads (torque), and degree of freedom, were applied to the model as the pinion rotated in an anti-clockwise direction. The center of the gear shaft was set in the longitudinal direction of the gear tooth surfaces. The value of load (torque) was applied to the gear for the same angular position of the pinion in each set. A non-linear static analysis with the Newton–Raphson method was used to estimate the contact stress and determine the maximum stress location. In the post-processing section, the Von Mises stress distribution technique was applied to obtain the stress in 10 increments. Figure 3 shows the procedure of the FEA simulation to determine the gear contact stress.

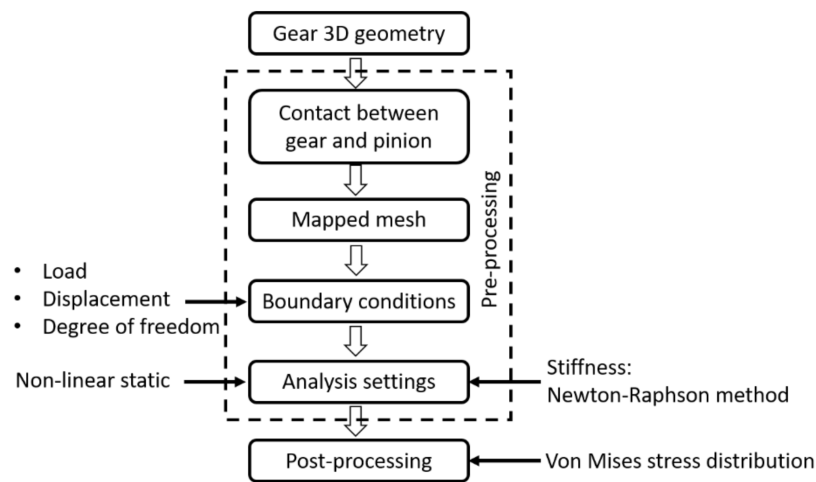


Figure 3. Block diagram showing the FEA simulation procedure to determine the gear contact stress.

Figure 4 shows the diagram of application of meshing and boundary conditions, and the position of maximum stress for both gear sets. The load (torque) was applied to the gear shaft, and the maximum stress was established at the teeth contact point of the gear and pinion. In order to perform a suitable stress analysis of the gear, the specifications of the two gear sets in the simulation were considered, as illustrated in Table 3.

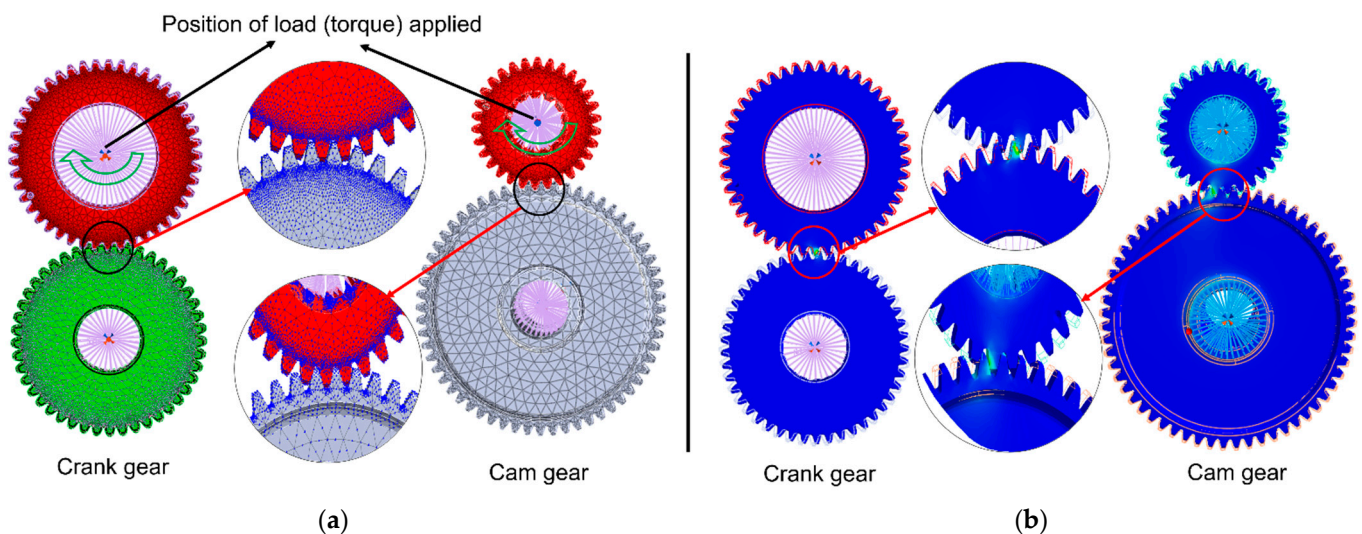


Figure 4. (a) Application of meshing and boundary conditions, and (b) position of the maximum stress.

Table 3. Picking device gear mechanism stress analysis to obtain the contact stress using FEA simulation.

| Parameter | Specification | | | |
|-------------------------------------|------------------------------|--------|--------------|--------|
| | Crank Gear Set | | Cam Gear Set | |
| | Gear | Pinion | Gear | Pinion |
| Number of teeth, integer | 45 | 45 | 30 | 60 |
| Pressure angle, degree (α) | 20 | 20 | 20 | 20 |
| Pitch circle diameter, mm | 47 | 47 | 32 | 64 |
| Base circle radius, mm | 22 | 22 | 15 | 30 |
| Addendum circle radius, mm | 24 | 24 | 17 | 33 |
| Radius of pitch circle, mm | 23.5 | 23.5 | 16 | 32 |
| Node, integer | 124,342 | 75,457 | 46,855 | 71,831 |
| Element, integer | 83,695 | 49,344 | 27,912 | 42,929 |
| Material | Medium- or high-carbon steel | | | |
| Operating condition | 2.95 Nm @ 6.284 rad/s | | | |

In order to encourage picking device gears to revolve continuously, the previous contact point of the gear teeth should be introduced before the current teeth–point contact is completed. The contact ratio represents the ratio of the average number of gear tooth pairs in contact for a pair of contact gears [16]. The contact ratio C_R was calculated using Equations (3)–(5).

$$C_R = \frac{l}{P_b} \quad (3)$$

$$l = \sqrt{r_{o2}^2 - r_{b2}^2} + \sqrt{r_{o1}^2 - r_{b1}^2} - (r_{p1} + r_{p2}) \times \sin \alpha_0 \quad (4)$$

The pitch of the base circle P_b is equal to the pitch P_n . Thus,

$$P_b = P_n = \pi \times m \times \cos \theta \quad (5)$$

Typically, the maximum contact ratio corresponds to the minimum stress as the contact load is distributed over the teeth. Here, the transmitting torque was assumed to be constant. The roll angle equivalent to the length of the contact path can be found by summing the approach angle and the recess angle. The roll angle (the angle corresponding to the length of the contact path) is defined in Equations (6)–(8) [36,37].

$$\varphi_C = \varphi_A + \varphi_R \quad (6)$$

$$\varphi_A = \frac{-S_A}{r_{b1}}, S_A = -r_{b1} \tan \theta + \sqrt{r_{o1}^2 - r_{b1}^2} \quad (7)$$

$$\varphi_R = \frac{S_B}{r_{b1}}, S_B = r_{b2} \tan \theta - \sqrt{r_{o1}^2 - r_{b1}^2} \quad (8)$$

2.2.3. Gear Contact Stress Analysis with AGMA Theory

In order to validate the results from the FEA, the stress was calculated from the measured load data using the AGMA theory [16,38]. While the gears and pinions transmit power, a high contact stress occurs at the tooth surface. Based on the AGMA stress theory, the gear contact stress was calculated for the contact between two cylinders [39]. The contact stress could be estimated using the face width of the gear, considering the allowable properties of the selected material. The contact stress at the tooth root between two mating gears was calculated based on the AGMA standard, using Equations (9) and (10).

$$F_m = \frac{2000T}{d_m} \quad (9)$$

$$\sigma_H = Z_E \sqrt{F_m K_o K_d K_s \frac{K_H}{2r_p 2F Z_1}} \quad (10)$$

2.3. Fatigue Life Prediction

Fatigue is a process that involves the cycle-by-cycle accumulation of damage in a material undergoing fluctuating stresses and strains. Failure occurs as a result of the accumulated damage level after a component experiences a certain number of load fluctuations [40]. The gear operating load of the transplanter picking device was analyzed by collecting the load signals as torque data. Figure 5 shows the load analysis procedure, determination of the load duration, and, finally, prediction of the fatigue life [24,41]. The load cycle counting method of the gears and bearings is different from the other machinery components [42]. To count the load cycles of gears and bearings, the load duration distribution (LDD) method is recommended based on ISO 10300 [41].

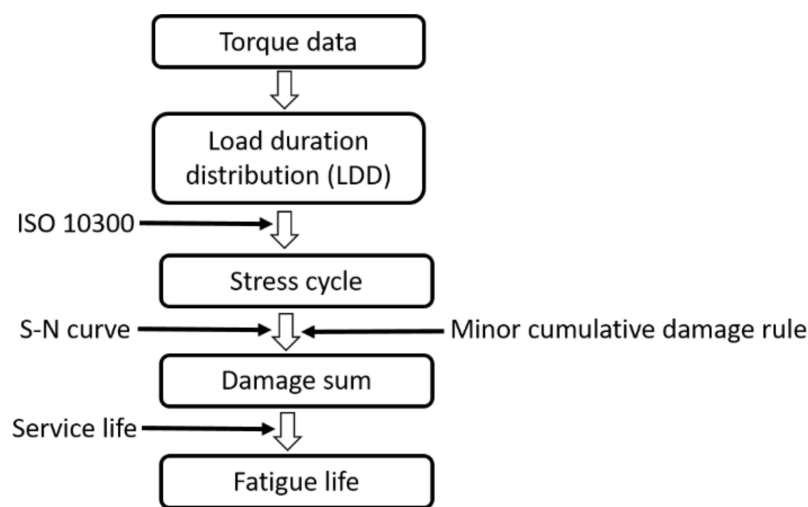


Figure 5. The procedure used to evaluate the fatigue life of the picking device gear. LDD: load duration distribution.

The counting of stress cycles of gears varies according to the external load cycles, and it is a function of the gear rotational speed [41]. The load cycles in every stress bin depend on the time duration and the gear rotational speed of the individual bin. Figure 6 shows the procedure of creating stress bins from load bins and load time series using the LDD method. The number of stress cycles was calculated using Equation (11).

$$N_T = 60 \frac{D_i}{D_t} N_i L \quad (11)$$

An S–N curve was converted to a torque–cycle curve, indicating the damage caused by the experiment [43]. The S–N curve was obtained for each of the tested gear materials using Equation (12).

$$N_c = 10^{(6 - 6.097 \log(\frac{\sigma_H}{225}))} \quad (12)$$

The Palmgren–Miner cumulative damage rule [44] was used to calculate the damage sum as in Equation (13). The lifespan of the transplanter was estimated as 10 years, and the annual usage time was 25.5 h [45]. The total life of the picking device gear was calculated by adding the percentage of life consumed at each stress level. The predicted fatigue life was calculated by dividing the lifespan of the transplanter and damage sum, as shown in Equation (14). The predicted fatigue life cycles were calculated using Equation (15). Table 4

summarizes the condition of the picking device gear mechanism according to the fatigue analysis.

$$D_t = \sum_{i=1}^k \frac{n_i}{N_c} \tag{13}$$

$$L_f = \frac{L_s}{D} \tag{14}$$

$$C_f = 60L_f N_c \tag{15}$$

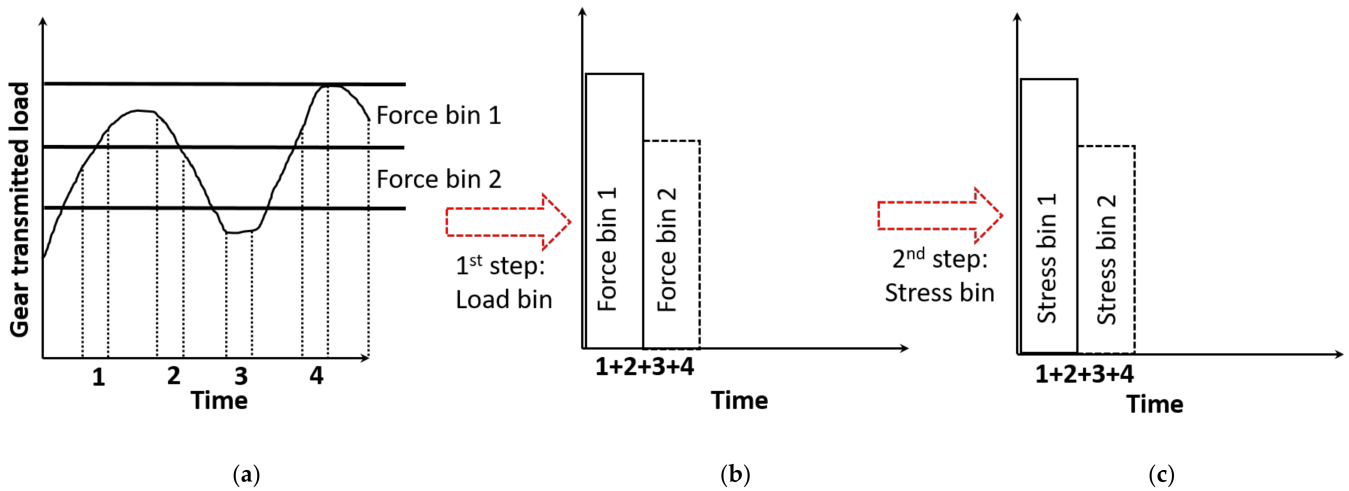


Figure 6. Stress bin calculation from load bins and load time series with the load duration distribution (LDD) method: (a) load curve, (b) load bins, and (c) stress bins.

Table 4. Condition of the picking device gear mechanism for the fatigue analysis.

| Parameter | Specification |
|-----------------------|--------------------------------------|
| Lifespan | 10 year |
| Annual usage | 25.5 h |
| Operating speed | 6.284, 7.331, 8.378, and 9.425 rad/s |
| Cycle counting method | Load duration distribution |

2.4. Experimental Setup

A test bench was fabricated to measure the load of the picking device gear. The picking device was synchronized with a bevel gear transmission system and motor driveline so that the motor could run the picking device at the recommended operating speed. A chain transmission system was also synchronized with the motor and the driveline [3]. A three-phase electric motor was used as an external power source for the direct load applied to the test bench. The rated power of the motor was 1.5 kW, the rated speed was 366.52 rad/s, and the frequency was 60 Hz. An inverter (SV-iG5A; LS ELECTRIC Co. Ltd., Anyang, Korea) with an on/off switch was used to control the angular velocity of the motor. The inverter rated power was 1.5 kW, and the rated voltage of the three-phase motor was 200 V. In order to determine the load of the picking operation, a torque sensor (TRS605; FUTEK Advanced Sensor Technology, Inc., California, CA, USA) was installed in the power driveline between the motor and the picking device. A data acquisition device (NI 6212; National Instruments Corp., Austin, Texas, TX, USA) and a software program (LabVIEW; National Instruments Corp., Austin, Texas, TX, USA) were used to acquire the sensor signal data [46]. The fabrication and instrument setup of the picking mechanism load measurement test bench are described in Figure 7. A set of tests were performed to determine the relationships between the load and the damage configuration. The underdeveloped automatic pepper transplanter was designed with a picking device gear mechanism operating speed of

6.284 rad/s. To investigate the load duration and fatigue life, the operating conditions for this test bench were selected as low speed (6.284 and 7.331 rad/s) and high speed (8.378 and 9.425 rad/s). The experiment was repeated five times, and the torque data were recorded separately for each experiment. Table 5 describes the considerations and the specifications of the stress and fatigue analysis experimental setup.

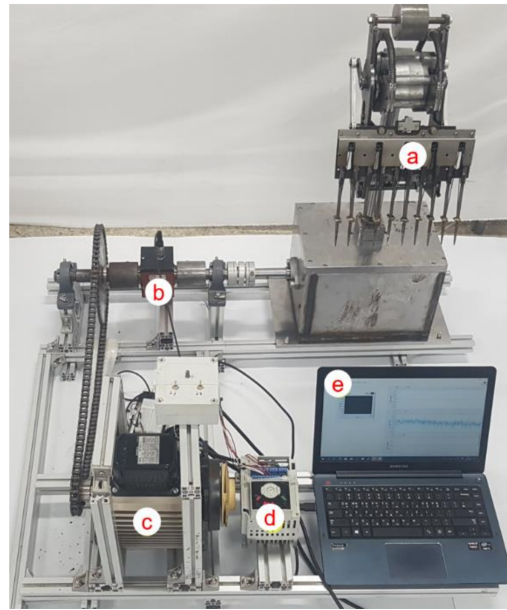


Figure 7. Load measurement test bench for the picking device: (a) picking device, (b) torque sensor, (c) motor, (d) inverter, and (e) data storage panel.

Table 5. Specifications of the stress and fatigue analysis experimental setup.

| Parameter | | Specification |
|----------------|------------------------|--------------------------------|
| Electric motor | Rated power, kW | 1.5 @ 366.52 rad/s |
| | Rated torque, Nm | 3.5 |
| | Operating speed, rad/s | 6.284, 7.331, 8.378, and 9.425 |

3. Results and Discussion

3.1. Appropriate Gear Material and Face Width

The Lewis bending stress theory was used to estimate face width range of the picking device gear sets for AISI 1060 steel and SCM 420H carbon steel materials. The allowable stress of the materials and operating conditions were considered to select the range of face widths as the thickness of the gear sets. Table 6 shows the face width range for different materials and operating speeds. For the allowable stress of AISI 1060 steel (high carbon steel) and SCM 420H carbon steel (medium carbon steel), the face width range of the gear set was found to be between 3 and 5 mm. Therefore, 3 and 5 mm face widths were considered for further stress analysis of the material of the picking device gear mechanism.

Figure 8 shows the load (torque) of the picking device gear mechanism for four different operating speeds. The torque on the picking device showed regular fluctuation patterns during operation. The average torque at 9.425 rad/s was approximately two-times higher than that at 6.284 rad/s. The maximum torque was found when the picking mechanism changed direction from the y- to the x-axis. The maximum torque was found to be 3.65 Nm for the 9.425 rad/s operating condition. The average torque values for the picking device at 6.284, 7.331, 8.378, and 9.425 rad/s were 0.17 ± 0.32 , 0.26 ± 0.33 , 0.28 ± 0.39 , and 0.32 ± 0.45 Nm, respectively. Therefore, the load on the picking device increased when the speed of the device increased, as expected.

Table 6. Determined picking device gear set face width based on the operating speed and material properties.

| Rotational Speed, rad/s | Face Width, mm | | | |
|-------------------------|-----------------|----------|-----------------------|----------|
| | AISI 1060 Steel | | SCM 420H Carbon Steel | |
| | Crank Gear | Cam Gear | Crank Gear | Cam Gear |
| 6.284 | 4.50 | 4.06 | 4.29 | 3.87 |
| 7.331 | 4.56 | 4.10 | 4.36 | 3.92 |
| 8.378 | 4.82 | 4.33 | 4.60 | 4.13 |
| 9.425 | 5.45 | 4.88 | 5.20 | 4.65 |

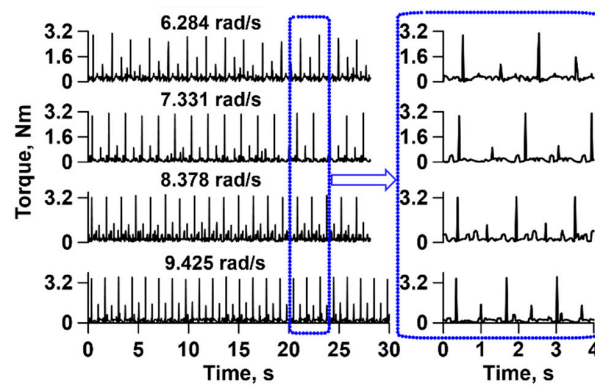


Figure 8. Picking device gear mechanism torque based on the operating speed.

The roll angle φ_C was calculated as 0.20 and 0.16 rad for the crank and cam gear sets, respectively. That is, the contact starts from 0 rad and ends at 0.20 and 0.16 rad for the crank and cam gear sets, respectively. The torque load was applied to the center of each gear. The contact stress on the pinion at the contact location was observed for various roll angles. Table 7 shows the maximum contact stress for the crank gear set under different load conditions, where the roll angle increased from 0.02 to 0.18 rad in 10 equal increments. In the FEA, tip relief was not considered, and the maximum stress levels for the full load condition at the contact location were obtained as 890.96 (Case 4), 613.78 (Case 5), 885.06 (Case 4), and 695.02 MPa (Case 6) for 3 and 5 mm face widths of SCM 420H carbon steel and AISI 1060 steel, respectively. While the gear and pinion are meshed and revolved, the stress reaches a maximum around the contact point corresponding to one pair of contacting teeth, and then reduces.

Table 7. Maximum stress obtained through contact stress analysis for the crank gear set.

| Load Type | Case | Roll Angle, rad | Crank Gear Set Maximum Stress, MPa | | | |
|-----------|--------------------|-----------------|------------------------------------|-----------------|-----------------|-----------------|
| | | | SCM 420H Carbon Steel | | AISI 1060 Steel | |
| | | | 3 mm Face Width | 5 mm Face Width | 3 mm Face Width | 5 mm Face Width |
| Half load | 1 | 0.02 | 137.65 | 177.39 | 149.16 | 203.93 |
| | 2 | 0.04 | 808.64 | 451.56 | 853.08 | 523.30 |
| | 3 | 0.06 | 855.48 | 519.96 | 890.97 | 636.33 |
| | 4 | 0.08 | 890.96 | 576.07 | 885.06 | 671.71 |
| Full load | 5 | 0.10 | 804.97 | 613.78 | 837.69 | 665.92 |
| | 6 | 0.12 | 631.63 | 597.10 | 700.32 | 695.02 |
| | 7 | 0.14 | 496.23 | 498.34 | 518.65 | 562.09 |
| | 8 | 0.16 | 318.29 | 321.68 | 335.30 | 410.71 |
| Half load | 9 | 0.18 | 228.34 | 262.58 | 242.62 | 278.18 |
| | 10 | 0.20 | 128.21 | 143.05 | 137.61 | 168.09 |
| Full load | AGMA (6.284 rad/s) | | 724.22 | 560.98 | 731.12 | 566.32 |

Table 8 shows the maximum contact stress for the cam gear set under different load conditions. The roll angle was increased from 0.01 to 0.15 rad in 10 equal increments. For the 3 and 5 mm face widths, the contact stress levels that the cam gear set were calculated as 620.63 and 480.74 and 626.54 and 485.31 MPa for SCM 420H carbon steel and AISI 1060 steel material, respectively. In the stress analysis using FEA, the contact stresses were 769.05 (Case 4), 567.04 (Case 5), 786.35 (Case 4), and 607.67 MPa (Case 6) for 3 and 5 mm face widths of SCM 420H carbon steel and AISI 1060 steel, respectively.

Table 8. Maximum stress obtained through contact stress analysis for cam gear set.

| Load Type | Case | Roll Angle, rad | Cam Gear Set Maximum Stress, MPa | | | |
|-----------|---------------|-----------------|----------------------------------|-----------------|-----------------|-----------------|
| | | | SCM 420H Carbon Steel | | AISI 1060 Steel | |
| | | | 3 mm Face Width | 5 mm Face Width | 3 mm Face Width | 5 mm Face Width |
| Half load | 1 | 0.01 | 151.05 | 147.17 | 155.23 | 151.00 |
| | 2 | 0.03 | 251.24 | 260.90 | 259.58 | 271.48 |
| | 3 | 0.04 | 575.63 | 504.17 | 630.88 | 580.26 |
| | 4 | 0.06 | 769.05 | 566.61 | 786.35 | 584.02 |
| Full load | 5 | 0.07 | 702.44 | 567.04 | 745.25 | 576.09 |
| | 6 | 0.09 | 710.74 | 522.31 | 701.26 | 607.67 |
| | 7 | 0.10 | 675.44 | 507.65 | 672.49 | 524.94 |
| Half load | 8 | 0.12 | 396.16 | 456.60 | 405.07 | 466.20 |
| | 9 | 0.13 | 265.14 | 291.71 | 283.62 | 303.83 |
| Full load | 10 | 0.15 | 173.74 | 199.77 | 184.79 | 211.27 |
| | AGMA | | | | | |
| | (6.284 rad/s) | | 620.63 | 480.74 | 626.54 | 485.31 |

From the stress analysis, the stresses in Cases 0 to 3 and 8 to 10 were not considered because they generated a drastic load (half load). In the full-load cases (4 to 7), the stress propagated diagonally and generated a maximum stress at the contact point. Cases 5 and 6 corresponded to the best-suited conditions among the full-load cases because they maintained the middle portion of the roll angle and applied stress more uniformly [16]. Based on the results, the SCM 420H carbon steel material showed the maximum stress in Cases 5 and 6.

From the comparison of FEA and AGMA theory contact stress, the highest error was found for a 3 mm face width for both materials. However, the lowest error was for the 5 mm face width of SCM 420H carbon steel. Therefore, a 5 mm face width of SCM 420H carbon steel was selected for the crank gear set to operate the picking mechanism. Similarly, for the cam gear analysis, the highest error was found for the 3 mm face in both materials. However, the lowest error was calculated for the 5 mm face width SCM 420H carbon steel. For the cam gear set, a 5 mm face width SCM 420H carbon steel would be suitable as the material for supporting the gear contact stress in field operation. Figure 9 shows the contact stress percentage error for the picking device gear mechanism.

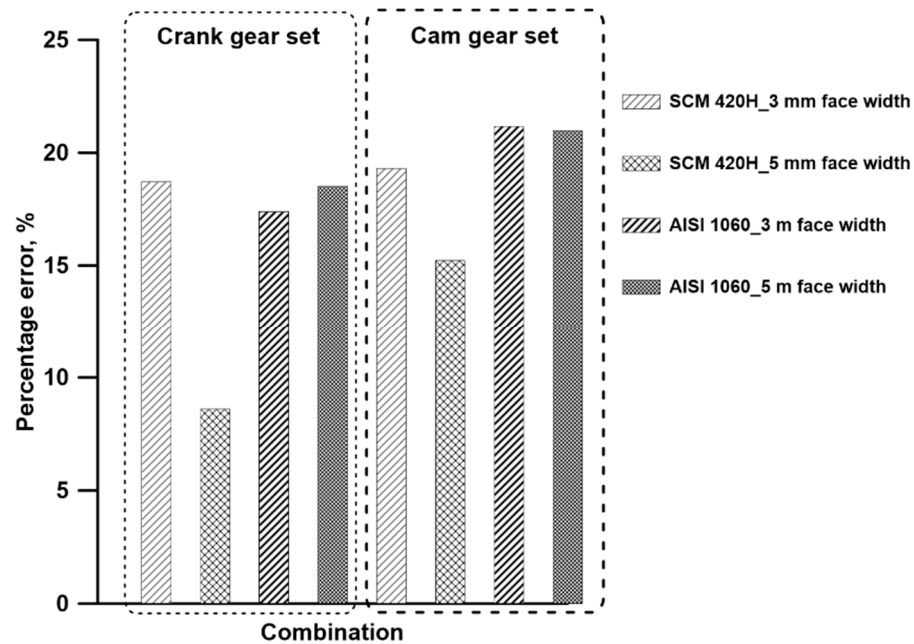


Figure 9. Contact stress percentage error for the picking device gear mechanism from the FEA and AGMA standard stress analysis.

3.2. Gear Mechanism Fatigue Life

Table 9 shows the load duration of the picking device gear mechanism with respect to operating speed. The maximum load duration was 1.75×10^5 h for the 6.284 rad/s condition, corresponding to a 10-year service life with a 95% total load. The maximum measured values of the torque range were from 2.96 to 3.55 Nm, and the maximum load durations were between approximately 3.61×10^4 and 1.75×10^5 h.

Table 9. Load duration of the picking device gear mechanism with respect to operating speed.

| Stress Bin | 9.425 rad/s | | 8.378 rad/s | | 7.331 rad/s | | 6.284 rad/s | |
|------------|-------------|-------------|-------------|-------------|-------------|-------------|-------------|-------------|
| | Torque, Nm | Duration, h |
| 1 | 0.18 | 36,133.50 | 0.21 | 30,982.50 | 0.12 | 176,205 | 0.22 | 175,567.50 |
| 2 | 0.67 | 892.50 | 0.63 | 6273 | 0.40 | 10,710 | 0.55 | 9562.50 |
| 3 | 1.38 | 255 | 1.24 | 280.50 | 0.97 | 2040 | 1.10 | 2550 |
| 4 | 1.45 | 408 | 1.36 | 255 | 1.21 | 255 | 0.00 | 0 |
| 5 | 0.00 | 0.00 | 0.00 | 0 | 0.00 | 0 | 1.64 | 1020 |
| 6 | 3.55 | 535.50 | 3.24 | 459 | 3.02 | 1912.50 | 2.96 | 1020 |

Figure 10 shows the predicted fatigue life of the picking device gear mechanism under different operating conditions. The most serious fatigue damage is shown at the 9.425 rad/s, because the gear was subjected to high loads under high operating speeds. According to the torque levels from the experiments at 9.425, 8.378, 7.331, and 6.284 rad/s, fatigue lifetimes for the cam mechanism gear were 1119.14, 1179.68, 1470.10, and 4635.97 h, respectively. On the other hand, the fatigue life for the crank mechanism gear was lower due to the high stress applied to the gear. For the crank gear set, predicted fatigue lifetimes were 436.65, 460.27, 573.58, 1808.80 h at 9.425, 8.378, 7.331, and 6.284 rad/s, respectively. The lifespan of the transplanter was estimated at 255 h. In this analysis, the predicted gear mechanism fatigue life was greater (by approximately two to 18 times) than the lifespan of the transplanter. It was indicated that the SCM 420H carbon steel material with a 5 mm gear face was suitable to operate the picking device for a service life of 10-years.

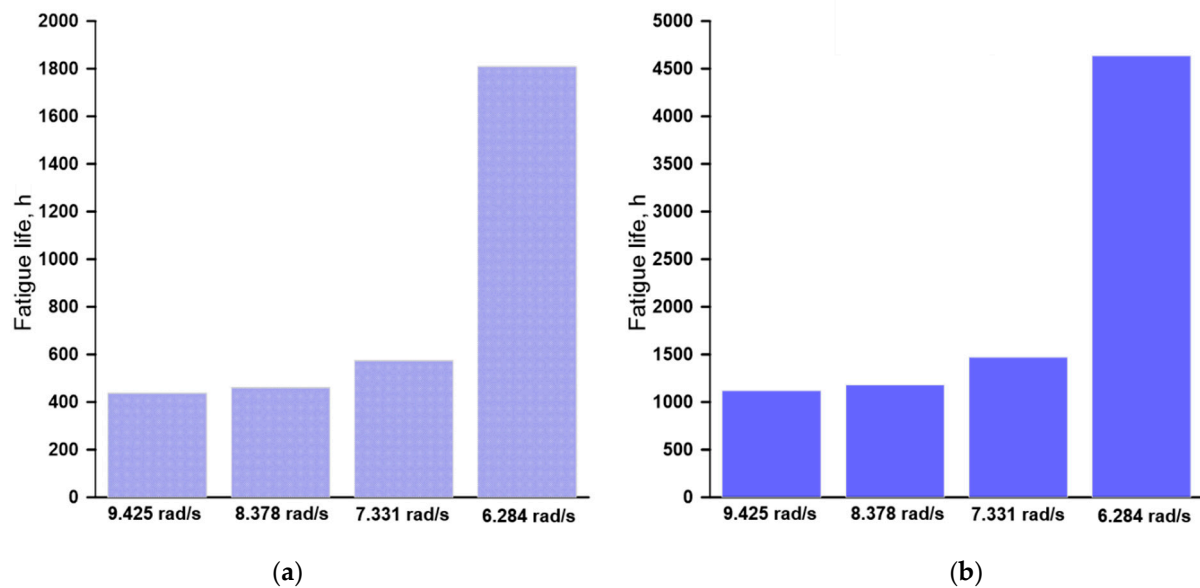


Figure 10. Predicted fatigue life hours of the picking device gear mechanism for the 10-year service life: (a) crank gear and (b) cam gear.

4. Conclusions

In this study, different materials and dimensions of an automatic pepper transplanter picking device gear mechanism were evaluated to identify those that achieved suitable gear mechanical properties using a non-linear FEA simulation and loads acting on a gear set. A torque measurement test bench was developed to analyze the load condition of the picking device gear under different operations. Based on the FEA simulation, the maximum stress value was observed at the contact point of the meshing gear and pinion. The stress analysis result also indicated that the high- and middle-carbon steel materials were appropriate for the design of this type of picking device gear mechanism. The high-carbon steel material was more expensive than the middle-carbon steel material, therefore it would increase the manufacturing cost. For example, a middle-carbon steel material (for example, SCM 420H carbon steel) with a carbon percentage of 0.25 to 0.60% could be used for the picking mechanism gear set. To evaluate the fatigue life of the gear, the damage was calculated using the load duration distribution method and S–N curve, based on torque data measured in the experiment. According to the fatigue analysis, the damage of the working load on the transmission increased with increasing gear speed, and the SCM 420H carbon steel with a 5 mm face width was suitable to operate the picking device for a 10-year (recommended) service life. The theoretical and experimental results of this study provide useful information for gear set design for an automatic pepper transplanter picking mechanism. In particular, the results can be used for designing optimal pepper transplanter transmissions, thereby improving design reliability and reducing material costs.

Author Contributions: Conceptualization, S.-O.C., and M.N.I.; methodology, S.-O.C., and M.N.I.; software, M.N.I.; validation, M.N.I., S.-O.C., and D.-H.L.; formal analysis, M.N.I., M.Z.I., and M.A.; investigation, S.-O.C., and M.S.N.K.; resources, S.-O.C.; data curation, M.N.I., M.Z.I., M.S.N.K., and M.A.; writing—original draft preparation, M.N.I.; writing—review and editing, S.-O.C., D.-H.L., and M.C.; visualization, M.N.I., M.Z.I., M.C., and K.S.; supervision, S.-O.C.; project administration, S.-O.C.; funding acquisition, S.-O.C. All authors have read and agreed to the published version of the manuscript.

Funding: This work was supported by the Korea Institute of Planning and Evaluation for Technology in Food, Agriculture, Forestry, and Fisheries (IPET) through the Advanced Production Technology Development Program, funded by the Ministry of Agriculture, Food, and Rural Affairs (MAFRA) (project no. 317013–03), Korea.

Institutional Review Board Statement: Not applicable.

Informed Consent Statement: Not applicable.

Data Availability Statement: The data presented in this study are available within the article.

Conflicts of Interest: The authors declare no conflict of interest.

References

1. Surh, Y.J.; Lee, E.; Lee, J.M. Chemoprotective properties of some pungent ingredients present in red pepper and ginger. *Mutat. Res. Mol. Mech. Mutagen.* **1998**, *402*, 259–267. [[CrossRef](#)]
2. Maia, A.A.D.; de Moraes, L.C. Kinetic parameters of red pepper waste as biomass to solid biofuel. *Bioresour. Technol.* **2016**, *204*, 157–163. [[CrossRef](#)] [[PubMed](#)]
3. Islam, M.N.; Iqbal, M.Z.; Ali, M.; Chowdhury, M.; Kabir, M.S.N.; Park, T.; Kim, Y.J.; Chung, S.O. Kinematic analysis of a clamp-type picking device for an automatic pepper transplanter. *Agriculture* **2020**, *10*, 0627. [[CrossRef](#)]
4. Dihingia, P.C.; Kumar, G.V.P.; Sarma, P.K. Development of a hopper-type planting device for a walk-behind hand-tractor-powered vegetable transplanter. *J. Biosyst. Eng.* **2016**, *41*, 21–33. [[CrossRef](#)]
5. Paraforos, D.S.; Griepentrog, H.W.; Vougioukas, S.G. Methodology for designing accelerated structural durability tests on agricultural machinery. *Biosyst. Eng.* **2016**, *149*, 24–37. [[CrossRef](#)]
6. Socie, D.; Pompetzki, M. Modeling variability in service loading spectra. *J. ASTM Int.* **2004**, *1*, 11561. [[CrossRef](#)]
7. Perozzi, D.; Mattetti, M.; Molari, G.; Sereni, E. Methodology to analyse farm tractor idling time. *Biosyst. Eng.* **2016**, *148*, 81–89. [[CrossRef](#)]
8. Margolin, L.G. Damage and failure in a statistical crack model. *Appl. Sci.* **2020**, *10*, 8700. [[CrossRef](#)]
9. Lee, Y.S.; Ali, M.; Islam, M.N.; Rasool, K.; Jang, B.E.; Kabir, M.S.N.; Kang, T.K.; Chung, S.O. Theoretical analysis of bending stresses to design a sprocket for transportation part of a chinese cabbage collector. *J. Biosyst. Eng.* **2020**, *45*, 85–93. [[CrossRef](#)]
10. Prabhakaran, S.; Ds, B. Stress analysis and effect of misalignment in spur gear stress analysis and effect of misalignment in spur gear. *Int. J. Appl. Eng. Res.* **2014**, *9*, 13061–13071.
11. Li, S. Effect of addendum on contact strength, bending strength and basic performance parameters of a pair of spur gears. *Mech. Mach. Theory* **2008**, *43*, 1557–1584. [[CrossRef](#)]
12. Pedrero, J.I.; Pleguezuelos, M.; Muñoz, M. Critical stress and load conditions for pitting calculations of involute spur and helical gear teeth. *Mech. Mach. Theory* **2011**, *46*, 425–437. [[CrossRef](#)]
13. Zhang, Y.; Fang, Z. Analysis of tooth contact and load distribution of helical gears with crossed axes. *Mech. Mach. Theory* **1999**, *34*, 41–57. [[CrossRef](#)]
14. Arafa, M.H.; Megahed, M.M. Evaluation of spur gear mesh compliance using the finite element method. *Proc. Inst. Mech. Eng. Part C J. Mech. Eng. Sci.* **1999**, *213*, 569–579. [[CrossRef](#)]
15. Pimsarn, M.; Kazerounian, K. Efficient evaluation of spur gear tooth mesh load using pseudo-interference stiffness estimation method. *Mech. Mach. Theory* **2002**, *37*, 769–786. [[CrossRef](#)]
16. Hwang, S.C.; Lee, J.H.; Lee, D.H.; Han, S.H.; Lee, K.H. Contact stress analysis for a pair of mating gears. *Math. Comput. Model.* **2013**, *57*, 40–49. [[CrossRef](#)]
17. Park, S.; Kim, S.; Choi, J.H. Gear fault diagnosis using transmission error and ensemble empirical mode decomposition. *Mech. Syst. Signal Process.* **2018**, *108*, 58–72. [[CrossRef](#)]
18. Kim, W.S.; Kim, Y.J.; Baek, S.M.; Moon, S.P.; Lee, N.G.; Kim, Y.S.; Park, S.U.; Choi, Y.; Kim, Y.K.; Choi, I.S. Fatigue life simulation of tractor spiral bevel gear according to major agricultural operations. *Appl. Sci.* **2020**, *10*, 8898. [[CrossRef](#)]
19. Berger, C.; Eulitz, K.-G.; Heuler, P.; Kotte, K.L.; Naundorf, H.; Schuetz, W.; Sonsino, C.; Wimmer, A.; Zenner, H. Betriebsfestigkeit in Germany—An overview. *Int. J. Fatigue* **2002**, *24*, 603–625. [[CrossRef](#)]
20. Kloth, W.; Stoppel, T. Kräfte, Beanspruchungen und Sicherheiten in den Landmaschinen. *Z. Ver. Dtsch. Ing.*, **1936**, *80*, 85–92.
21. Harral, B.B. The application of a statistical fatigue life prediction method to agricultural equipment. *Int. J. Fatigue* **1987**, *9*, 115–118. [[CrossRef](#)]
22. Kim, J.H.; Kim, K.U.; Wu, Y.G. Analysis of transmission load of agricultural tractors. *J. Terramechanics* **2000**, *37*, 113–125. [[CrossRef](#)]
23. Graham, J.A.; Berns, D.K.; Olberts, D.R. Cumulative damage used to analyze tractor final drives. *Trans. ASAE* **1962**, *5*, 139–146. [[CrossRef](#)]
24. Kim, Y.J.; Chung, S.O.; Choi, C.H. Effects of gear selection of an agricultural tractor on transmission and PTO load during rotary tillage. *Soil Tillage Res.* **2013**, *134*, 90–96. [[CrossRef](#)]
25. Lee, D.H.; Kim, Y.J.; Chung, S.O.; Choi, C.H.; Lee, K.H.; Shin, B.S. Analysis of the PTO load of a 75 kW agricultural tractor during rotary tillage and baler operation in Korean upland fields. *J. Terramechanics* **2015**, *60*, 75–83. [[CrossRef](#)]
26. Kim, J.H.; Kim, K.U.; Choi, C.W.; Wu, Y.G. Severeness of transmission loads of agricultural tractors. *J. Biosyst. Eng.* **1998**, *23*, 417–426.
27. Mattetti, M.; Molari, G.; Sereni, E. Damage evaluation of driving events for agricultural tractors. *Comput. Electron. Agric.* **2017**, *135*, 328–337. [[CrossRef](#)]
28. Bai, J.; Wu, X.; Gao, F.; Li, H. Analysis of powertrain loading dynamic characteristics and the effects on fatigue damage. *Appl. Sci.* **2017**, *7*, 1027. [[CrossRef](#)]

29. Al-Tubi, I.S.; Long, H.; Zhang, J.; Shaw, B. Experimental and analytical study of gear micropitting initiation and propagation under varying loading conditions. *Wear* **2015**, *328–329*, 8–16. [[CrossRef](#)]
30. Chen, Y.C.; Tsay, C.B. Stress analysis of a helical gear set with localized bearing contact. *Finite Elem. Anal. Des.* **2002**, *38*, 707–723. [[CrossRef](#)]
31. Litvin, F.L.; Lian, Q.; Kapelevich, A.L. Asymmetric modified spur gear drives: Reduction of noise, localization of contact, simulation of meshing and stress analysis. *Comput. Methods Appl. Mech. Eng.* **2000**, *188*, 363–390. [[CrossRef](#)]
32. Lisle, T.J.; Shaw, B.A.; Frazer, R.C. External spur gear root bending stress: A comparison of ISO 6336:2006, AGMA 2101-D04, ANSYS finite element analysis and strain gauge techniques. *Mech. Mach. Theory* **2017**, *111*, 1–9. [[CrossRef](#)]
33. Townsend, D.P.; Coy, J.J.; Zaretsky, E.V. Experimental and analytical load-life relation for AISI 9310 steel spur gears. *J. Mech. Des. Trans. ASME* **1978**, *100*, 54–60. [[CrossRef](#)]
34. Hewitt, J. Design and materials selection for power-transmitting gears. *Mater. Des.* **1992**, *13*, 230–238. [[CrossRef](#)]
35. Choi, J.C.; Choi, Y. Precision forging of spur gears with inside relief. *Int. J. Mach. Tools Manuf.* **1999**, *39*, 1575–1588. [[CrossRef](#)]
36. Litvin, F.L. *Gear Geometry and Applied Theory*, 3rd ed.; Cambridge University Press: Cambridge, UK, 2004.
37. Hassan, A.R. Contact stress analysis of spur gear teeth pair. *World Acad. Sci. Eng. Technol.* **2009**, *58*, 597–602.
38. Achari, A.; Sathyanarayana, R.P. Chaitanya, and S.P. A comparison of bending Stress and contact stress of a helical gear as calculated by AGMA standards and FEA. *Int. J. Emerg. Technol. Adv. Eng.* **2014**, *4*, 38–43.
39. Karpat, F.; Ekwaro-Osire, S.; Cavdar, K.; Babalik, F.C. Dynamic analysis of involute spur gears with asymmetric teeth. *Int. J. Mech. Sci.* **2008**, *50*, 1598–1610. [[CrossRef](#)]
40. Kadhim, N.A.; Mustafa, M.; Varvani-Farahani, A. Fatigue life prediction of low-alloy steel samples undergoing uniaxial random block loading histories based on different energy-based damage descriptions. *Fatigue Fract. Eng. Mater. Struct.* **2015**, *38*, 69–79. [[CrossRef](#)]
41. Nejad, A.R.; Gao, Z.; Moan, T. On long-term fatigue damage and reliability analysis of gears under wind loads in offshore wind turbine drivetrains. *Int. J. Fatigue* **2014**, *61*, 116–128. [[CrossRef](#)]
42. Nejad, A.R.; Xing, Y.; Guo, Y.; Keller, J.; Gao, Z.; Moan, T. Effects of floating sun gear in a wind turbine's planetary gearbox with geometrical imperfections. *Wind Energy* **2015**, *18*, 2105–2120. [[CrossRef](#)]
43. Nguyen, H.T.; Chu, Q.T.; Kim, S.E. Fatigue analysis of a pre-fabricated orthotropic steel deck for light-weight vehicles. *J. Constr. Steel Res.* **2011**, *67*, 647–655. [[CrossRef](#)]
44. Miner, M.A. Cumulative damage in fatigue. *J. Appl. Mech.* **1945**, *12*, 159–164.
45. Kim, W.S.; Kim, Y.S.; Kim, Y.J.; Choi, C.H.; Inoue, E.; Okayasu, T. Analysis of the load of a transplanter PTO shaft based on the planting distance. *J. Fac. Agric. Kyushu Univ.* **2018**, *63*, 97–102. [[CrossRef](#)]
46. Iqbal, M.Z.; Islam, M.N.; Chowdhury, M.; Islam, S.; Park, T.; Kim, Y.J.; Chung, S.O. Working speed analysis of the gear-driven dibbling mechanism of a 2.6 kw walking-type automatic pepper transplanter. *Machines* **2021**, *9*, 6. [[CrossRef](#)]